Microstructural and dielectric properties of KCl-added bismuth vanadate ceramics

K. Shantha and K. B. R. Varma*

Materials Research Centre, Indian Institute of Science, Bangalore-560 012, India

The effect of KCl addition on the microstructural, structural and dielectric properties of bismuth vanadate, $Bi_2VO_{5.5}$ (BiV) has been examined. The average grain size of BiV ceramics increases with increase in KCl content (from an average grain size of 10 to 80 μm) as a result of the increased liquid-phase formation of KCl, at the grain boundaries. Differential scanning calorimetry (DSC) carried out on the KCl-added samples indicates an upward shift in the transition temperature (T_c), from 723 K (for BiV) to 734 K (for 5 mol% KCl-added BiV). On further increase in the KCl content, T_c shifts down to about 722 K for 10 mol%. This trend is consistent with that of the lattice strain data. The relative permittivity as well as the dielectric loss decrease by more than half of the original values upon the addition of KCl. The relative permittivities of the KCl-added ceramics are comparable with the values predicted by the logarithmic mixture rule. Impedance analyses suggest that the grain boundary resistance of the KCl-added BiV ceramics is higher by two orders of magnitude than that of BiV ceramics. The KCl-added BiV ceramics exhibit ferroelectric domains and the domain density decreases as the grain boundary region is approached.

Materials belonging to the Aurivillius family[1] of oxides, with the general formula $(Bi_2O_2)^{2+}(A_{n-1}B_nO_{3n+1})^{2-}$, are of special interest by virtue of their high relative permittivities and promising electro-optic properties.[2–4] Bismuth vanadate, $Bi_2VO_{5.5}$ (BiV), has a crystal structure that is similar to that of the $n=1$ member of this homologous series and it is reported to be orthorhombic and ferroelectric at 300 K.[5–8] While the polar properties of this compound are promising, the dielectric loss tangent ($\tan\delta$) values, both at 300 K and at T_c, are high (0.3 at 300 K and 3.5 at T_c at 100 kHz[9]) which restricts its application for various ferroelectric devices. The high dielectric loss, due to the high ionic conductivity associated with the tetragonal phase of this compound, is undesirable from the ferroelectric and pyroelectric measurements viewpoint. The dielectric behaviour of BiV ceramics depends strongly on their microstructure and hence on the sintering conditions. The relative permittivity was found to increase steadily with increase in grain size.[10] It is known that the microstructural features including the grain size, grain-to-grain contact and the grain boundary layers of ferroelectric ceramics can be modified by suitable additives.[11–13] To improve the sintering process of the ceramics and to modify their microstructure, partial liquid-phase sintering is often employed.[13–15] The strategy adopted here, is to employ a material which not only provides a partial liquid medium to enhance the sintering process, but also helps in lowering the dielectric loss. For this purpose we have chosen potassium chloride (KCl), which is an off-valent ionic material in the present context, and hence is presumed to segregate at the grain boundaries and helps in minimising the intergranular interaction and consequently reduce the dielectric loss. Here, we report the results concerning the influence of KCl addition on the microstructural, structural and dielectric properties of BiV ceramics.

Experimental

Polycrystalline BiV powder was synthesised from a stoichiometric mixture of bismuth oxide, Bi_2O_3, and vanadium pentoxide, V_2O_5, *via* the mixed oxide solid-state reaction route. The preparative conditions have been reported elsewhere.[8] Formation of the phase has been confirmed by X-ray powder diffraction (XRD) studies. The pattern could be indexed to an orthorhombic cell, with unit cell parameters [so-called supercell parameters] $a_0=16.586$, $b_0=5.607(1)$, $c_0=15.276(3)$ Å, by taking the superlattice reflections into account. The finely ground powder of polycrystalline BiV (particle size ranging from 5 to 10 μm) was mixed with various molar concentrations of KCl in a ball mill for 2 h. They were pelletised at 300 K at a pressure of 30×10^4 kg m^{-2} and subsequently, sintered at 1020 K for 24 h. XRD studies were carried out on the powdered samples of the sintered pellets using Cu-Kα radiation. The surface of the ceramic sample, normal to the pressing axis, was also analysed by XRD, to investigate the possible occurrence of any preferential grain orientation. The internal strain was computed by monitoring the line broadening and line shift of a few selected peaks. The density of the sintered pellets was determined by liquid displacement method, using xylene ($\rho=0.87$ g cm^{-3}) and water ($\rho=1$ g cm^{-3}) as liquid media. The density and porosity values were computed according to the procedure outlined in our earlier paper.[16] Microstructural features were studied using a Cambridge S360 scanning electron microscope and grain size measurements were carried out using the line intercept method,[17] in which a grid of lines is superimposed on the micrograph. The average grain size is the ratio of the length of test lines sampled to the number of intersections with the grain boundaries counted. Quantitative elemental analysis was carried out using a LINK AN10000 energy dispersive X-ray analyser (EDX) employing ZAF-4 software. Differential scanning calorimetry (DSC) was performed on the powdered samples (the mean particle size lies in the range of 8 μm for BiV to 50 μm for 10 mol% KCl-added samples) of the sintered pellets, using a 910 thermal analyser, Dupont instruments. In the convention used here for reporting the DSC data, downward deflections indicate endothermic reactions and upward deflections indicate exothermic reactions. Initially, the sintered pellets were ground to the desired dimensions (1.78 mm in thickness and 12 mm in diameter) to perform measurements of relative permittivity. The dimensions of all the samples for dielectric study were maintained strictly to be the same. The capacitance and the impedance measurements were performed on these pellets as a function of frequency (100 Hz–10 MHz), at a signal strength of 0.5 V (rms), using an HP 4194A impedance/gain-phase analyser in conjunction with an in-house built high-temperature cell. For this purpose, gold electrodes were sputtered on either side of the sintered pellets and subsequently silver epoxy was used to bond the leads to these samples.

Results and Discussion

Microstructure

Fig. 1(*a*)–(*d*) depict the scanning electron micrographs of the as-sintered pellets of BiV, 1 mol%, 5 mol% and 10 mol%

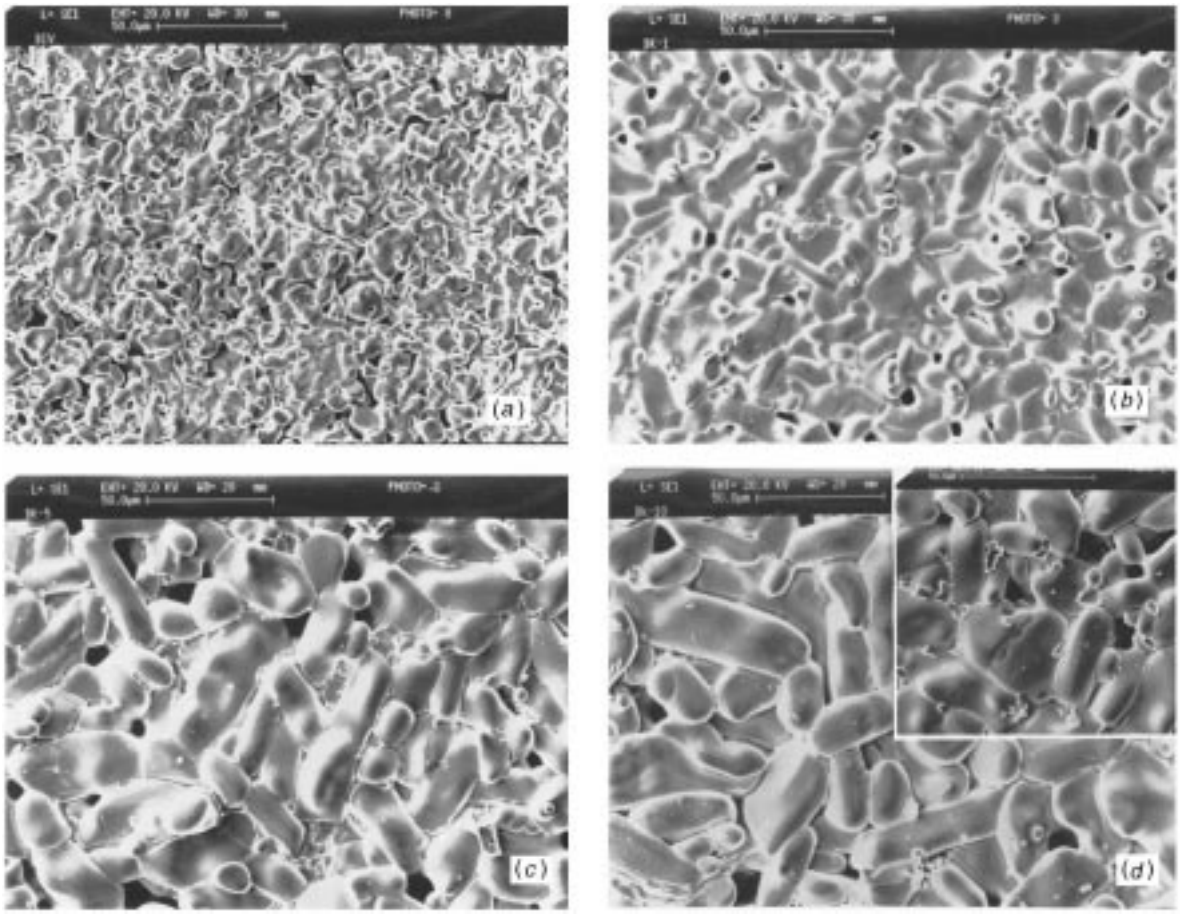

Fig 1 Scanning electron micrographs obtained for the thermally etched samples of (*a*) 0 mol%, (*b*) 1 mol%, (*c*) 5 mol% and (*d*) 10 mol% KCl added to BiV. [The inset of Fig. 1(*d*) shows the KCl crystallites dispersed at the grain boundaries.]

KCl-added BiV ceramics. The average grain size increases with increase in KCl content. Indeed, it varies from 10 μm (for BiV) to >80 μm (for BiV with 10 mol% KCl). It is evident from these micrographs that KCl addition enhances the grain growth. The enhanced grain growth encountered here is believed to be due to the liquid-phase formation of KCl, especially at the grain boundaries, during sintering. The presumption of liquid-phase formation of KCl is substantiated by the observation of solidified molten KCl in the intergranular regions [Fig. 2(*a*)] and the presence of dendritic structures [Fig. 2(*b*)] found mostly on the large grains (for KCl concentration $\geqslant 20$ mol%). This feature is a characteristic of recrystallisation from the melt. The EDX analysis of the dendrites indicates their composition to be predominantly KCl with trace amounts of Bi and V. The microstructural studies along with the EDX analyses carried out on KCl-added BiV samples, indicate no K or Cl on the grains but the presence of well developed prismatic shaped crystals of KCl at the grain boundaries [inset of Fig. 1(*d*)]. The formation of such prisms of the second phase is expected when the dihedral angle ϕ, between the faces, is close to 90°.[15] In the regions where ϕ tends to zero, at equilibrium, the faces of the grains are completely separated by the second phase. This leads to a build-up of the capillary pressure and a consequent enhancement in the diffusion rate, resulting in large grains. The increase in the grain size and the evolution of some chlorine are expected to lead to an increase in the intragranular porosity. Indeed the porosity of these samples, calculated based on the density data, demonstrates an increasing trend with increase in the concentration of the second phase (Fig. 3). A closer look at the morphological features of the grains in these ceramics, suggests the probable occurrence of grain orientation. Such elongated grains of large aspect ratio, have also been observed in the grain-oriented ceramics of strontium barium niobate,[18] bismuth tungstate,[19] bismuth titanate,[20] *etc.*

Chemically etched [dilute HNO_3 (1:4)] KCl-added ceramics, when subjected to SEM studies, revealed the presence of ferroelectric domains. Fig. 4(*a*) and (*b*) show the domain patterns obtained for BiV and 8 mol% KCl-added samples. The domain pattern of the KCl-added ceramic is strikingly different from that of BiV. The magnified versions of these patterns are shown as the insets for comparison. Also, the domains of the KCl-added samples are mostly confined to the central regions of the grains owing to the segregation of KCl, preferentially, to the grain boundaries.

XRD analysis

The XRD patterns recorded for BiV, 5 mol% and 10 mol% KCl-added BiV samples are shown in Fig. 5(*a*)–(*c*). Since the most intense Bragg peaks for KCl [$d=3.146$ Å ($I/I_0=1$), $d=2.225$ Å ($I/I_0=0.68$)] slightly overlap with those of BiV [$d=3.121$ Å ($I/I_0=1$) and $d=2.239$ Å ($I/I_0=0.08$)] , it was difficult to distinguish them. However, a slow scan has revealed the presence of the most intense peak of KCl (indicated by asterisk) and its intensity was found to increase with increase in the KCl content. The diffraction patterns obtained for BiV samples with KCl concentration $\geqslant 20$ mol% are strikingly different from the above patterns. Fig. 6 shows the X-ray powder diffraction pattern of 20 mol% KCl-added BiV ceramic. Careful analysis of this data indicates the presence of more than one phase. The X-ray peaks could be identified with those of $Bi_{12}V_2O_{23}$ (which is known to be a stable phase[21] in the binary phase diagram of Bi_2O_3–V_2O_5), KVO_3 and BiOCl. This observation suggests that KCl at higher concentrations ($\geqslant 20$ mol%)

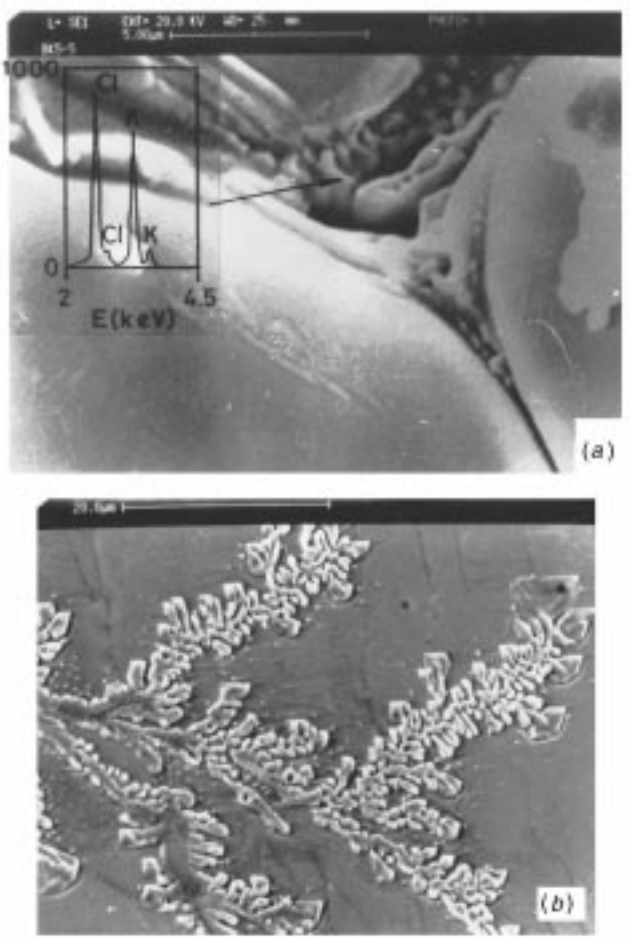

Fig 2 Scanning electron micrographs obtained for KCl added to BiV ceramics (*a*); the inset shows the EDX pattern obtained at the grain boundary; (*b*) shows the dendritic growth

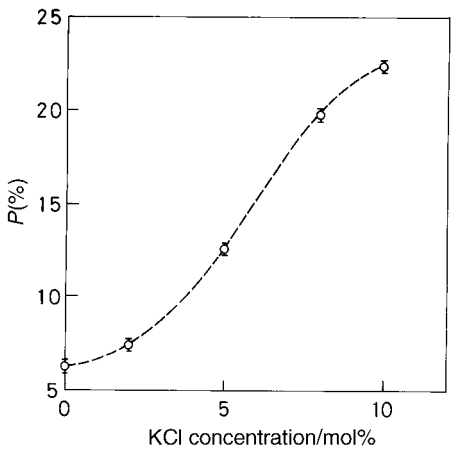

Fig 3 Variation of porosity with KCl concentration

probably reacts with BiV and gives rise to $Bi_{12}V_2O_{23}$, KVO_3 and BiOCl phases according to reaction (1).

$$8Bi_2VO_{5.5} + 6KCl \rightarrow Bi_{12}V_2O_{23} + 6KVO_3 + 4BiOCl + Cl_2\uparrow \quad (1)$$

The above equation is chemically balanced with respect to the cations.

The XRD patterns recorded for the sintered pellets exhibit intense (00*l*) reflections, confirming that the BiV grains are oriented with their *c*-axes along the pressing direction. The Lotgering orientation factor *f*, a measure of the degree of

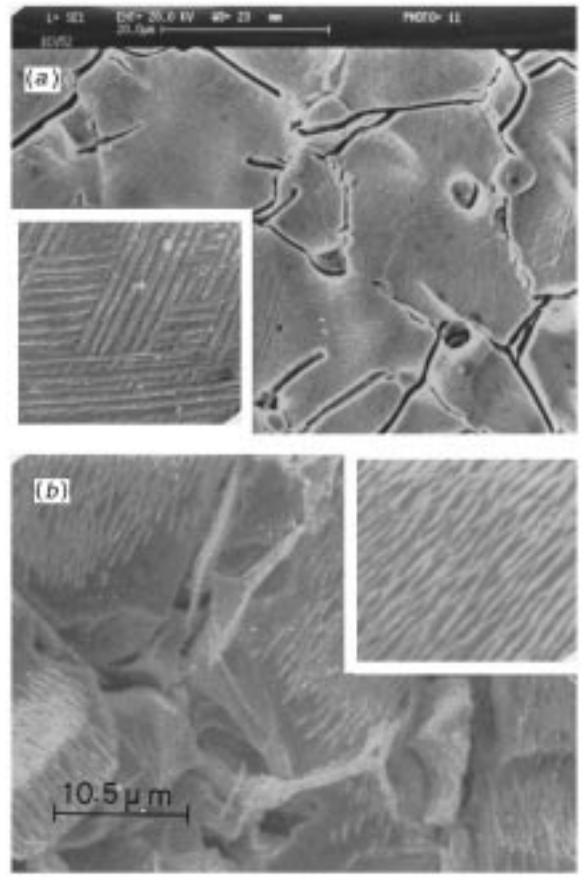

Fig 4 Scanning electron micrographs of chemically etched samples of (*a*) 0 mol% and (*b*) 5 mol% KCl-added BiV

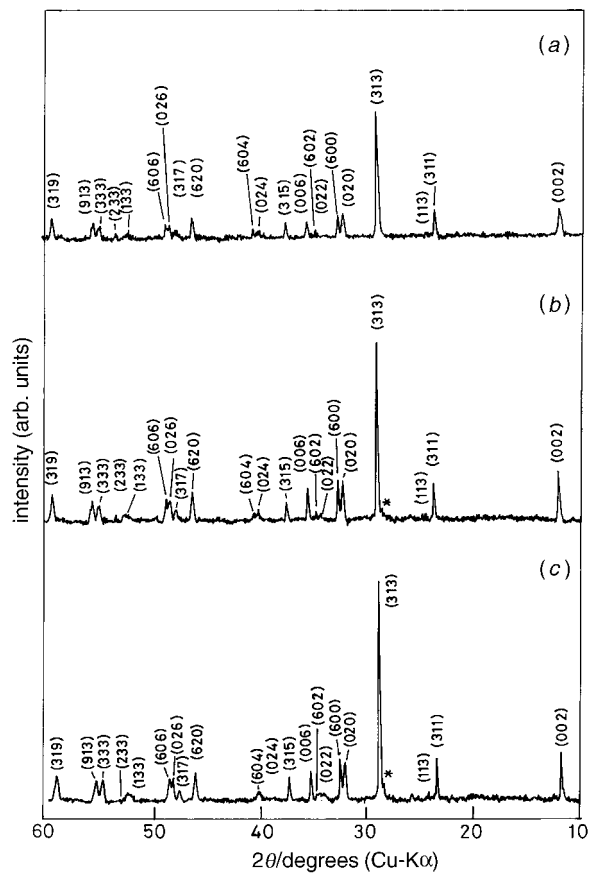

Fig 5 X-Ray powder diffraction patterns obtained for KCl added to BiV samples: (*a*) 0 mol%, (*b*) 5 mol% and (*c*) 10 mol%

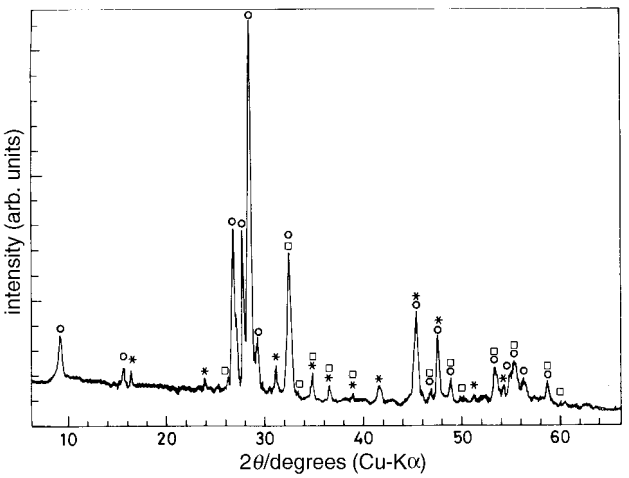

Fig 6 X-Ray powder diffraction pattern obtained for 20 mol% KCl added to BiV (*, KVO_3; ○, $Bi_{12}V_2O_{23}$; □, BiOCl)

orientation[22] is given by eqn. (2)

$$f=\frac{(p-p_0)}{(1-p_0)} \quad (2)$$

where $p=\sum I_{00l}/\sum I_{hkl}$ for the given oriented sample and $p_0=\sum I_{00l}/\sum I_{hkl}$ for the non-oriented sample were computed for all the samples. The orientation factor was found to be <0.4 for the above samples. However, the orientation was found to increase ($f\geqslant 0.72$), by subjecting the samples to repeated grinding and sintering. Detailed studies, to establish the influence of grain orientation on the physical properties, are in progress. The lattice parameters *a*, *b* and *c* were determined using a least-squares fit method (HOCT program—a linear least-squares fit for hexagonal, orthorhombic, cubic and tetragonal crystal systems). The *b*/*a* ratio, which is indicative of the orthorhombic distortion, plotted as a function of KCl concentration (Fig. 7), shows an increasing trend up to 5 mol% and then decreases subsequently. By contrast, the *c*/*a* ratio decreases up to 5 mol%, and thereafter increases. These changes may be due to the change in the internal strain present in these ceramics. When BiV is cooled below the transition temperature (tetragonal→orthorhombic), the volume change that is likely to be associated with the phase transformation, will eventually generate a slight lattice deformation of its constituent orthorhombic BiV crystallites. As a consequence the volume change for one crystallite can be inhibited by the surrounding crystallites. In the present case, since almost all the grain boundaries consist of KCl crystallites of varied sizes, it is more likely that it can create an additional lattice strain. An attempt was made to evaluate the lattice strain using the X-ray line-broadening method.[23] A plot of $\beta\cos\theta$ *vs.* $\sin\theta$ was generated and the strain involved has been computed based on the slope obtained. Here, $\beta=\Delta\theta_c+\Delta\theta$ and $\Delta\theta_c$ is the full width at half maximum (FWHM) of the peak at the Bragg angle θ (radians) and $\Delta\theta$ is the shift in the peak position. The (311), (020) and (600) peaks were considered for these calculations. The internal strain decreases initially with increase in porosity (*P*), up to $P=12\%$ (corresponding to 5 mol% of KCl). This is expected because of the fact that pores generally act as buffers and reduce the strain in ceramics.[24] Subsequently, the internal strain increases with increase in porosity (Fig. 8). This anomalous increase in the internal strain, beyond 5 mol% of KCl, may be due to the dominant role played by KCl crystallites (which are significantly large both in number and size, at higher concentrations of KCl) in inhibiting the volume change of BiV crystallites. On the other hand, a change in the lattice parameters may also be due to the slight solubility of KCl in BiV. However, a systematic EDX analysis did not reveal the presence of K or Cl in the interior of the grains. Therefore, it is conjuctured that the contribution, from the possible formation of solid solution between KCl and BiV, to the lattice parameter change may not be significant.

Differential scanning calorimetry

DSC studies carried out on these samples indicate that the transition temperature (T_c) shifts towards higher values up to 5 mol% of KCl and with further increase in the KCl content it decreases. Fig. 9 shows the variation of T_c with KCl concentration. This variation is consistent with the variation in the internal strain (Fig. 8). As the internal strain decreases initially

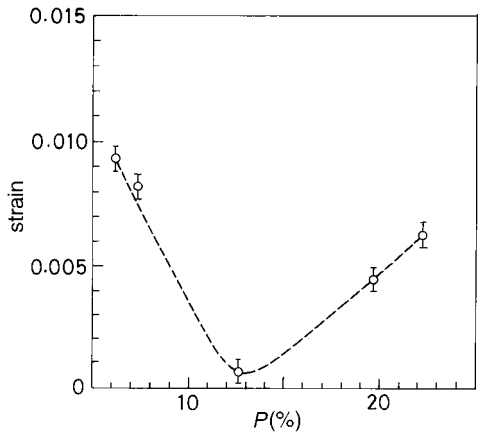

Fig 8 Variation of the lattice strain as a function of the porosity of the KCl-added ceramics

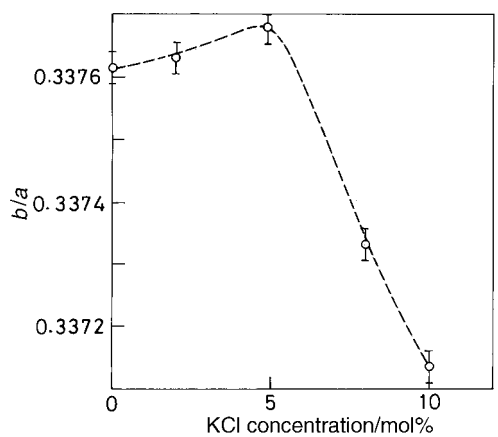

Fig 7 Variation of the *b*/*a* ratio as a function of KCl concentration

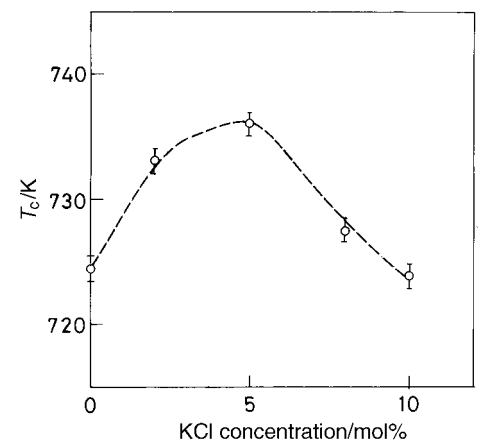

Fig 9 Variation of T_c as a function of KCl concentration

up to 5 mol% of KCl, T_c increases and then as the strain increases, T_c decreases. Also, the variation of the b/a ratio is consistent with that of the T_c (Fig. 7).

Dielectric characterization

The relative permittivity (ε_r) and the loss tangent ($\tan\delta$) obtained as a function of frequency at 300 K for BiV, 2 mol%, 5 mol% and 10 mol% KCl-added BiV ceramics are summarised in Fig. 10 and 11. The value of ε_r, in all the cases, was found to decrease with increasing frequency (up to 10 MHz). However, the fall in ε_r is rapid up to 10 kHz and subsequently the dispersion is not high (inset of Fig. 10). The values of ε_r as well as $\tan\delta$ decrease with increase in KCl content at all the frequencies under study. The variation of ε_r as a function of KCl concentration, at 10 kHz, is shown in Fig. 12. SEM, EDX and XRD investigations confirm the presence of the KCl phase in the BiV matrix and porosity calculations yield non-negligible porosity values. Hence, we have made an attempt to understand the dielectric behaviour of this three-phase system using the logarithmic mixture rule,[25] according to which the total relative permittivity ε_r, expressed in terms of the volume fractions v_i and the relative permittivities $(\varepsilon_r)_i$ of the constituent phases, is given by eqn. (3)

$$\log \varepsilon_r = \sum_i v_i \log (\varepsilon_r)_i \qquad (3)$$

In order to estimate the individual volume fractions of the three phases, the samples were weighed in three different media:

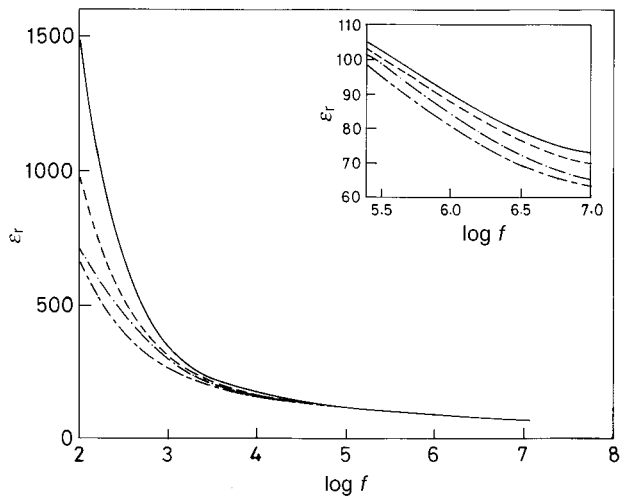

Fig 10 Variation of ε_r with frequency, for BiV samples with different concentrations of KCl (—, 0; – – –, 2; –·–, 5; –··–, 10 mol% KCl)

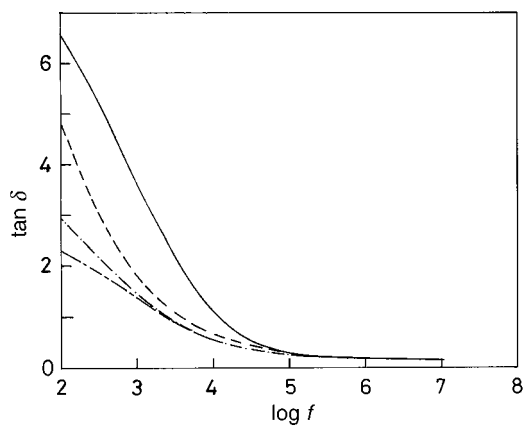

Fig 11 Frequency variation of $\tan\delta$, for BiV samples with different concentrations of KCl (—, 0; – – –, 2; –·–, 5; –··–, 10 mol% KCl)

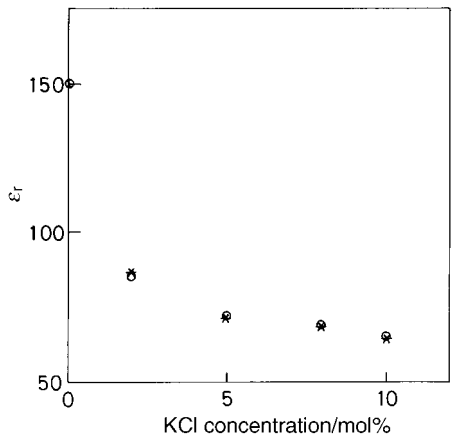

Fig 12 Variation of ε_r as a function of KCl concentration (○); the values obtained from logarithmic mixture rule are also depicted (*)

air, xylene and water. With increase in KCl concentration, the volume fraction of BiV decreases, whereas the volume fractions of the other two phases (KCl and porosity) increase. The relative permittivity values at 10 kHz predicted by the logarithmic mixture rule, for all the samples under study, are in close agreement with those obtained experimentally (Fig. 12). These results suggest a random distribution of KCl crystallites in the BiV matrix.

It is clear from Fig. 11 that $\tan\delta$ could significantly be reduced, by more than half its original value, by adding a nominal amount (5 mol%) of KCl to the BiV ceramic. Thus, it can be concluded that the presence of KCl, particularly at the grain boundaries (as evidenced by the SEM studies) of BiV ceramics, minimises the grain-to-grain contact, and helps in reducing the dielectric loss. The decrease in $\tan\delta$ (or in otherwards electrical conductivity) may also be due to the increase in the intragranular porosity with increase in grain size. This reduced conductivity might help in establishing the true ferroelectric behaviour of BiV ceramics. In fact, the preliminary results obtained in this direction are promising and the full details of this work will form a separate publication.

The dielectric properties monitored as a function of temperature (300–800 K), at various frequencies show that ε_r and $\tan\delta$ both at 300 K and at T_c, for the KCl-added samples are lower than those of BiV. Fig. 13 shows the variation in ε_r, of 5 mol% KCl-added BiV ceramic, as a function of temperature at various frequencies. The transition temperature (T_c) obtained by the relative permittivity measurements closely matches with that obtained *via* DSC studies.

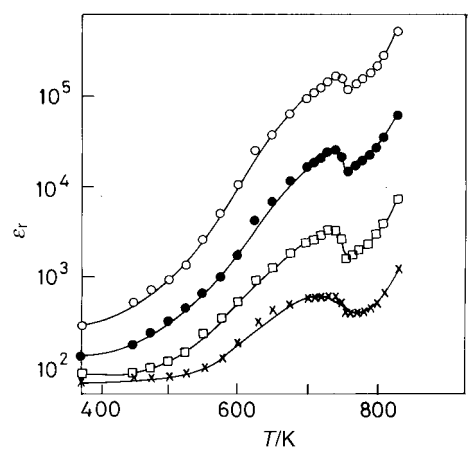

Fig 13 Temperature dependence of ε_r, for the 5 mol% KCl-added sample, at various frequencies (○, 100 Hz; ●; 1 kHz; □, 10 kHz; ×, 100 kHz)

The strong low-frequency dielectric dispersion (LFDD) in the frequency response of ε_r (Fig. 10), similar to that observed in parent BiV can be rationalised by invoking Jonscher's dielectric model.[26–30] According to Jonscher's dielectric dispersion relation, the real part of the relative permittivity is given by eqn. (4)

$$\varepsilon_r' = \varepsilon_\infty + \frac{a(T)}{\varepsilon_0} \sin\left[n(T)\frac{\pi}{2}\right] \omega^{n(T)-1} \quad (4)$$

where ε_∞ is the 'high frequency' value of the relative permittivity, $n(T)$ is the temperature-dependent exponent, which determines the 'strength of the ion–ion coupling [small values of $n(T)$ corresponding to strongly interacting systems] and $a(T)$ determines the 'strength' of the polarizability arising from the universal mechanism in question. By curve-fitting the experimental dielectric data to the above equation, the exponent $n(T)$ and the parameter $a(T)$ can be determined. Fig. 14 shows a close fit obtained between the experimental and the theoretical data for a 5 mol% KCl-added BiV sample both at 300 K and at high temperatures. However, the $n(T)$ values in this case are lower than those of BiV, while the $a(T)$ values are higher. In fact, both the parameters exhibit anomalies at T_c (similar to those observed in BiV),[31] indicating a coupling between the charge carriers and the phonons.

Impedance measurement

Fig. 15(*a*) and (*b*) show the complex impedance spectra of BiV and 5 mol% KCl-added BiV samples, recorded at 550 K. The spectra could be resolved into overlapping arcs associated with the grain and grain boundary responses. At the low-frequency end, an additional arc with an associated capacitance in the μF range is observed, which is attributed to the electrode–sample interfacial effect.[32] By analysing the complex impedance spectra, the resistance and the capacitance of the grain and the grain boundaries were determined. Table 1 lists the grain and the grain boundary resistance R_g, R_{gb} and capacitance C_g and C_{gb}, respectively, for BiV and 5 mol% KCl-added BiV ceramics. The values of the grain and the grain boundary capacitance obtained in the present study for BiV sample are in the same range as reported by Lee *et al.* [32]

It can be noted from Table 1, that the grain boundary resistance of the KCl-added sample is two orders of magnitude higher than that of BiV sample, whereas its grain boundary capacitance C_{gb} is lower. This explains the lowering of the ε_r and tan δ values in the KCl-added ceramics.

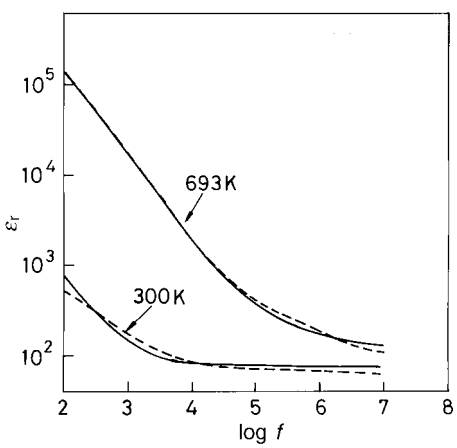

Fig 14 Frequency variation of the relative permittivity for the 5 mol% KCl-added sample, at two different temperatures, along with the theoretical values obtained by Jonscher's universal dispersion relationship (—, theoretical fit; – – –, experimental)

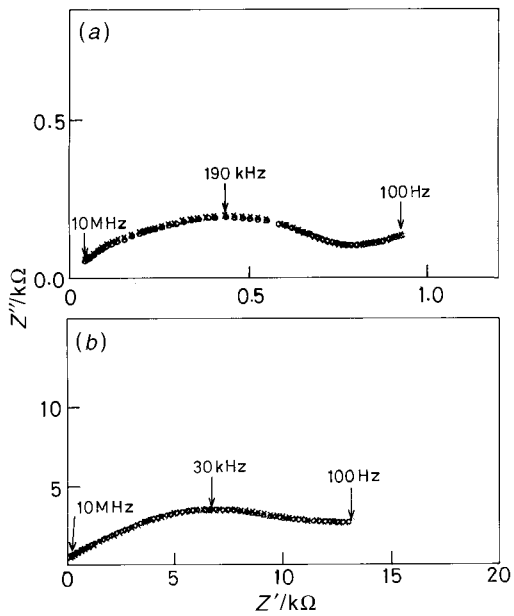

Fig 15 Complex impedance spectra of (*a*) 0 mol% and (*b*) 5 mol% KCl-added to BiV samples, recorded at 550 K (●, measured; ×, simulated)

Table 1 Resistance and capacitance measurements for BiV and BiV + 5 mol% KCl

sample	R_g/Ω	R_{gb}/Ω	C_g/F	C_{gb}/F
BiV	3×10^2	5.8×10^2	4.7×10^{-10}	1.0×10^{-7}
BiV + 5 mol% KCl	7×10^4	1.46×10^4	1.4×10^{-10}	5.8×10^{-8}

Conclusions

BiV ceramics containing various concentrations of KCl have been fabricated and the correlation between the microstructural and dielectric properties has been established. These ceramics exhibit an increase in the grain size with increase in KCl content. The internal strain and the b/a ratio (which is a measure of the orthorhombic distortion) vary with KCl concentration and exhibit an anomaly near 5 mol%, resulting in a corresponding shift in T_c. The SEM, EDX and XRD studies indicate the presence of KCl crystallites in the BiV matrix. Further, the relative permittivity of these samples could be predicted based on the logarithmic mixture rule. The decrease in the relative permittivity as well as the dielectric loss with increasing KCl content, is attributed to the segregation of KCl at the grain boundaries.

The authors thank Mr Sam Philip for his help in carrying out the SEM studies.

References

1 B. Aurivillius, *Ark. Kemi.*, 1949, **1**, 463; 1949, bf **1**, 499; 1950, **2**, 519.
2 S. E. Cummins and B. H. Hill, *Proc. I.E.E.E.*, 1970, **58**, 938.
3 T. E. Luke, *I.E.E.E. Trans.*, 1969, **ED-16**, 576.
4 S. E. Cummins, *J. Phys. Soc. Jpn.*, 1970, **28**, 396.
5 A. A. Bush and Yu. N. Venevtsev, *Russ. J. Inorg. Chem.*, 1986, **31**, 769.
6 V. G. Osipian, L. M. Savchenko, V. L. Elbakyan and P. B. Avakyan, *Inorg. Mater.*, 1987, **23**, 467.
7 V. N. Borisov, Yu. M. Poplavko, P. B. Avakyan and V. G. Osipyan, *Sov. Phys. Solid State*, 1988, **30**, 904.
8 K. B. R. Varma, G. N. Subbanna, T. N. Guru Row and C. N. R. Rao, *J. Mater. Res.*, 1990, **5**, 2718.
9 K. V. R. Prasad and K. B. R. Varma, *J. Phys. D. Appl. Phys.*, 1991, **24**, 1858.
10 K. V. R. Prasad and K. B. R. Varma, *J. Mater. Sci.*, 1994, **29**, 2691.

11 B. Jimenez, R. G Polledo, C. Alemany, J. Mendiola and E. Maurer, *Ferroelectrics*, 1976, **14**, 687.
12 J. Portelles, I. Gonzalez, A. Kiriev, F. Calderon and S. Garcia, *J. Mater. Sci. Lett*., 1993, **12**, 1871.
13 S. Nishiwaki, J. Takahashi and K. Kodaira, *Jpn. J. Appl. Phys*., 1994, **33**, 5477.
14 L. Lü, M. O. Lai and G. Li, *Mater. Res. Bull*., 1996, **31**, 453.
15 W. D. Kingery, H. K. Bowen and D. R. Uhlmann, *Introduction to Ceramics*, John Wiley and Sons, New York, 1976.
16 K. Shantha, Sam Phillip and K. B. R. Varma, *Mater. Chem. Phys*., in press.
17 G. F. Vander Voort, *Applied Metallography*, Van Nostrand Reinhold Company, New York, 1986.
18 K. Nagata, Y. Yamamoto, H. Igarashi and K. Okazaki, *Ferroelectrics*, 1981, **38**, 853.
19 T. Kimura, M. H. Holmes and R. E. Newnham, *J. Am. Ceram. Soc*., 1982, **65**, 223.
20 T. Takenaka and K. Sakata, *Jpn. J. Appl. Phys*., 1980, **19**, 31.
21 Wuzhong Zhou, *J. Solid State Chem*., 1988, **76**, 290.
22 F. K. Lotgering, *J. Inorg. Nucl. Chem*., 1959, **9**, 113.
23 K. Gurumurugan, D. Mangalaraj, Sa. K. Narayandass, K. Sekar and C. P. Girija Vallabhan, *Semicond. Sci. Technol*., 1994, **9**, 1.
24 H. I. Hsiang, F. S. Yen and C. Y. Huang, *Jpn. J. Appl. Phys*., 1995, **34**, 1922.
25 V. K. Lichteneker, *Phys. Z*, 1926, **27**, 115.
26 A. K. Jonscher, *Nature* (*London*), 1977, **267**, 673.
27 A. K. Jonscher, *Dielectric Relaxation in Solids*, Chelsea Dielectric Press, London, 1983.
28 L. A. Dissado and R. M. Hill, *J. Chem. Soc., Faraday Trans*., 1985, **81**, 2480.
29 A. K. Jonscher, *J. Mater. Sci*., 1989, **24**, 372.
30 K. Shantha and K. B. R. Varma, *Solid State Ionics*, in press.
31 Z. Lu, J. P. Bonnet, J. Ravez and P. Hagenmuller, *Solid State Ionics*, 1992, **57**, 235.
32 C. K. Lee, D. C. Sinclair and A. R. West, *Solid State Ionics*, 1993, **62**, 193.

Paper 6/06965G; *Received* 11*th October*, 1996